Clim. Past Discuss., 2, 371–397, 2006
www.clim-past-discuss.net/2/371/2006/

Climate of the Past Discussions

Climate of the Past Discussions is the access reviewed discussion forum of *Climate of the Past*

Quasi-100 ky glacial-interglacial cycles triggered by subglacial burial carbon release

N. Zeng

Department of Atmospheric and Oceanic Science, and Earth System Science Interdisciplinary Center, University of Maryland, USA

Received: 22 May 2006 – Accepted: 13 June 2006 – Published: 7 July 2006

Correspondence to: N. Zeng (zeng@atmos.umd.edu)

Abstract

A new mechanism is proposed in which climate, carbon cycle and icesheets interact with each other to produce a feedback that can produce quasi-100 ky glacial-interglacial cycles. A key process is the burial and preservation of organic carbon by icesheets. The switch from glacial maximum to deglaciation is triggered by the ejection of glacial burial carbon when icesheets grow to sufficiently large size and subglacial transport becomes significant. Glacial inception is initiated by CO_2 drawdown due to a "rebound" from a high but transient interglacial CO_2 value as the land-originated CO_2 invades into deep ocean via thermohaline circulation and $CaCO_3$ compensation. Also important for glacial inception is the CO_2 uptake by vegetation regrowth in the previously ice-covered boreal regions. When tested using a fully coupled Earth system model with comprehensive carbon cycle components and semi-empirical physical climate components, it produced self-sustaining glacial-interglacial cycles of duration about 93 ky, CO_2 change of 90 ppmv, temperature change of 6°C under certain parameter regimes. Since the 100 ky cycles can not be easily explained by the weak Milankovitch astronomical forcing alone, this carbon-climate mechanism provides a strong feedback that could interact with external forcings to produce the major observed Quaternary climatic variations.

1 Introduction

Paleoclimatic evidence from ice cores, ocean sediments and other sources reveal oscillations in climate and atmospheric CO_2 over the last million years, with major signals in 20, 41 and 100 ky (thousands of years) frequency bands (Hays et al., 1976; Petit et al., 1999; EPICA, 2004). While changes in solar radiation caused by perturbations to Earth's orbit appear to be directly responsible for the 20 ky and 41 ky cycles, the explanation of the dominant 100 ky cycles remains elusive (Imbrie et al., 1993; Roe and Allen, 1999; Wunsch, 2004).

CPD

2, 371–397, 2006

Glacial cycles triggered by burial carbon release

N. Zeng

EGU

It is increasingly clear that internal feedbacks in the Earth's climate system play a major role in the 100 ky cycles, whether it is pacemaked by orbital forcing or not. Atmospheric model simulations show that the 80–100 ppmv lower CO_2 is the dominant factor in producing about 5°C cooler glacial climate, with additional contribution from ice-albedo and other effects (Broccoli and Manabe, 1987; Lorius et al., 1990; Weaver et al., 1998). It is very difficult, if not impossible, to simulate the observed glacial cooling in comprehensive models without changing CO_2. Thus carbon-climate interaction may provide key internal feedbacks that have rarely been included in comprehensive models interactively.

Somewhat in parallel, when given the observed climate change, one can try to explain the glacial-interglacial atmospheric CO_2 change, but it has not been fully understood (Broecker and Henderson, 1998; Archer et al., 2000; Sigman and Boyle, 2000). Understanding the glacial CO_2 problem is emerging as the key in the 100 ky climate cycles (Saltzman and Maasch, 1988; Gildor and Tziperman, 2001; Ruddiman, 2003; Paillard and Parrenin, 2004). Among the competing and mostly ocean-based mechanisms, a more recent hypothesis (Zeng, 2003) proposes a different sign in terrestrial carbon change from glacial to interglacial by including organic carbon buried under the icesheets, thus contributing to the deglacial CO_2 increase. This together with other active oceanic mechanisms can explain the full amplitude of the observed CO_2 change.

Such a different terrestrial scenario would require the reexamination of a large amount of observations and theoretical ideas. One example is the marine C13 records that suggest terrestrial carbon storage increase from glacial maximum to integlacial (Curry et al., 1988). However, alternative explanations (at least possibilities) exist in which a lower glacial terrestrial carbon storage is not required (Spero et al., 1997). In addition, a terrestrial carbon release at deglaciation may offer more straightforward explanation to a number of perplexing issues such as the deglacial minimum and the transient behavior observed in the atmospheric and surface ocean C13 records (Smith et al., 1999; Spero and Lea, 2002; Zeng, 2003). The possible constraints need to be considered are beyond the scope here. Although the glacial burial hypothesis is not yet proven, it opens the door to some new possibilities that may be of value to the unsolved 100 ky problem.

2 Theory

Here I include some ingredients from the glacial burial hypothesis in a fully coupled carbon-climate-icesheet framework, rather than considering carbon cycle or climate separately with the other as forcing. An important new element is the hypothesis that the glacial burial carbon would be transported out of the icesheets when icesheet is sufficiently large, thus providing a switch mechanism to transit the system from glacial maximum to interglacial. The theory is outlined as following.

During glaciation (Fig. 1a), the cooling drives down atmospheric CO_2 through carbon storage in the ocean due to several effects such as lower sea surface temperature (SST), and on land due to lower soil decomposition rate, as well as vegetation growth on exposed continental shelves. The lowering CO_2 would further reduce temperature through weaker greenhouse effect. While oceanic CO_2 change is also influenced by many other factors such as plankton productivity, the land and ocean changes described above consist a well-known CO_2-temperature feedback. A main addition here from the glacial burial hypothesis (Zeng, 2003) is that during glaciation, vegetation and soil carbon accumulated around the preceding interglacial in the boreal region is buried and preserved under the major Northern Hemisphere icesheets.

When icesheets grow long enough and reach certain size, the buried carbon is transported out of the icesheets at the edges (Fig. 1b). This dead carbon may have been significantly transformed, but would nonetheless be released back into the atmosphere. If the release of this carbon is fast enough to outcompete the oceanic buffering effects, CO_2 would accumulate in the atmosphere and leads to rising CO_2, which would warm the atmosphere and melt icesheets, and this leads to further release of glacial burial carbon as well as continental shelf carbon (Fig. 1c). With also the help of CO_2-temperature and ice-albedo feedbacks, the system could get into a runaway deglaciation.

The deglaciation ends at interglacial when the major icesheets are melted away and the major "independent" carbon sources, namely glacial burial and continental shelf carbon are finished. If the deglacial land CO_2 release is faster than or comparable to the oceanic buffering timescales, in particular, the deep ocean invasion timescale of 1 ky and the $CaCO_3$ compensation timescale of 10 ky (Archer et al., 1997; Sigman and Boyle, 2000; Zeng, 2003), the interglacial would only be transient as atmospheric CO_2 would relax back towards an equilibrium value, analogous to the ocean uptake of the anthropogenic CO_2 pulse. In the meantime, regrowth in the boreal region after icesheets retreat would also take CO_2 out of the atmosphere. With the help of various positive feedbacks, this CO_2 drawdown would drive the system into a glacial inception (Fig. 1d), followed by further glaciation, thus completing one cycle.

3 Modeling approach

An Earth system model with balanced complexity in the components has been used to quantify the above theory. At present, it is not possible to run sophisticated GCMs for such long-term integration. The physical climate components we use are "semi-empirical" by interpolating GCM-simulated climate time slices (Kutzbach et al., 1998) and reconstructed icesheet distributions for the last 21 ky (Peltier, 1994). The interpolation weighting factor is determined by time-dependent CO_2, ice cover and topography. The carbon cycle models for both land and ocean are mechanistic. The details of the model components are provided in the appendix.

In the "semi-empirical" atmosphere model, precipitation and temperature simulated by CCM1 (Kutzbach et al., 1998) for the Holocene (6 kBP) are used as the model's interglacial maximum (Im), while its LGM (21 ky BP) simulation is used as glacial maximum (Gm). Thus the physical atmosphere is represented by a single time-dependent weighting factor $w(t)$ in addition to the spatial distributions at Gm and Im. For instance, temperature $T(x, t)$ can be computed as a linear interpolation between the two spatially varying extreme states $T_{Im}(x)$ and $T_{Gm}(x)$ simulated by CCM1 with w as the weighting factor:

$$T = wT_{Im} + (1 - w)T_{Gm} \tag{1}$$

where t is time and x represents the spatial dimensions, and $w{=}w(t)$ is a function of time only.

The climate factor w is determined by three independent factors as:

$$w = 0.5w_c + 0.3(1 - w_i) + 0.2(1 - w_h) \tag{2}$$

where w_c is the contribution from the greenhouse effect of atmosphere CO_2, w_i is due to ice-albedo feedback of the icesheets, and w_h is related to atmospheric circulation changes caused by the topographical height of the icesheets. The relative importance of these three factors were chosen to be 50%, 30%, and 20%, based on various estimates of the relative roles of greenhouse gases and icesheets (Broccoli and Manabe, 1987; Lorius et al., 1990; Weaver et al., 1998).

Ice cover change w_i is assumed to follow temperature change. The ice distribution information is based on the paleo ice cover and topography data of Peltier (1994) at 1 ky time resolution. However, unlike the straightforward interpolation for temperature and precipitation which can also be extrapolated, ice cover is either 0 or 1. Ice cover "interpolation" is therefore done by spreading (glaciation) or shrinking (deglaciation) the ice cover based on the information of w_i. Ice volume grows towards a potential value determined by the LGM data of Peltier (1994) and current ice cover w_i.

For the ocean, factors such as seaice, ocean circulation are fast changing and are treated as part of the physical atmosphere-ocean-land climate system which responds to greenhouse gas and icesheet forcing. Since we are concerned about the interaction between carbon cycle and climate, we only need to represent the effects of changes in the physical climate system on the carbon cycle. A sea surface temperature (SST) anomaly is slaved to the atmosphere with a time delay of 100 year. Since it is not the purpose here to include all the active ocean mechanisms, a change of ocean temperature by 6K at Gm was used as a surrogate of all the mechanisms. A major caveat is that this approach will not resolve significant timing differences of different ocean CO_2 mechanisms, which is beyond the scope of this work. Sensitivity experiment showed that this 6K SST effect alone produces about 55 ppmv glacial-interglacial CO_2 change, a value on the low side of which the major oceanic mechanisms can explain. This SST anomaly, along with the land-atmospheric carbon flux from the terrestrial carbon model VEGAS are given to the oceanic carbon model SUE (Ridgwell, 2001) which also computes atmosphere-ocean carbon exchange and atmospheric CO_2 which is then used by the physical atmosphere and land photosynthesis module. The terrestrial carbon model was described in Zeng (2003), and a fuller description of all the model components is included in the Appendix.

4 Results

The fully coupled carbon-climate-icesheet model was first run for 10 ky at an interglacial equilibrium, and it produced an equilibrium CO_2 level of 272 ppmv (Fig. 2). Atmospheric CO_2 was then artificially taken out of the system at a rate of 0.015 Gt y^{-1} for the next 26 ky, corresponding to a cumulative 390 Gt (Gigaton, or 10^{15} g) carbon sink. The system was then left to run by itself without any external forcing.

This CO_2 sink was enough to bring the system into a glaciation which continued due to the positive feedbacks in the system. A glacial maximum was reached, followed by several deglaciation and glaciation cycles until the end of the simulation. After the first two cycles in which the model had to adjust from the artificial CO_2 sink, the system settled into quasi-steady glacial-interglacial cycles with a period of 93 ky. The details over one cycle are shown in Fig. 3 and the mechanisms for the self-sustaining cycles are discussed below.

From interglacial to early glaciation, vegetation regrowth in the boreal region leads to accumulation of vegetation and soil carbon which is later buried under ice. While regrowth contributes to most of the early land carbon increase, carbon accumulation on exposed continental shelves dominates during late glaciation. At glacial maximum,

CPD
2, 371–397, 2006

Glacial cycles triggered by burial carbon release

N. Zeng

EGU

land carbon storage reaches highest value at about 2000 Gt.

Glacial maximum in the model is determined as ice volume reaches the maximum value. At this point, in addition to a normally slow height gradient dependent basal flow, the tall icesheets which are likely half melting at the base would produce significantly accelerated subglacial sediment transport through processes such as subglacial river runoff and fast flowing ice streams. Given the many unknowns on these processes, the model simply adds an additional transport to the burial organic carbon towards the edge of the icesheets at a speed increasing from zero to 8×10^{-6} m s^{-1} within 3000 years.

A turning point takes place few hundred years after the initial ejection of carbon out of the icesheets, when the decomposed burial carbon accumulates in the atmosphere enough to reverse the CO_2 decreasing trend. Once CO_2 starts to increase, climate warms, and several positive feedbacks act to further increase CO_2, including increasing SST and warming-induced release of active land carbon.

The model simulates two major periods of increasing CO_2 during deglaciation: an early (and continuing) increase in response to the release of glacial burial carbon, and a later period when continental shelves lose carbon as sea level rises. These can be seen clearly in the two deglacial peaks in the land-atmosphere carbon flux (Fig. 3 and Fig. 4). The deglacial increase in CO_2 is about 90 ppmv, while temperature increase is 6°C and deglaciation lasts about 7 ky.

The relative contribution to deglacial atmospheric CO_2 change is about 55 ppmv from ocean, and 45 ppmv from land, as indicated by two sensitivity experiments (Fig. 4). These add to 100 ppmv, 10 ppmv larger than the 90 ppmv change in the fully coupled run, because the ocean buffering effect is less effective at higher CO_2 in the land only case. Thus land contribution is close to 35 ppmv (inferred as a residual), slightly larger than the 30 ppmv found in Zeng (2003) where burial carbon was released in situ, in contrast to the basal flow induced faster land carbon release here.

Interglacial maximum with highest CO_2 and temperature is brief, followed immediately by CO_2 drawdown and cooling over the next 10 ky. The initial CO_2 decrease

CPD
2, 371–397, 2006

is rapid, mostly caused by a "rebound" (not to be confused with glacial isostatic rebound) from the fast deglacial CO_2 increase as land-originated CO_2 invades into deep ocean and by $CaCO_3$ compensation which have timescales of 1 ky and 10 ky, respectively. This interpretation is strengthened by a CO_2 drawdown of about 10 ppmv at early glacial inception even in the "positive land" flux only case (Fig. 4), despite the lack of any CO_2 uptake by land and active ocean mechanisms. It is seen clearly in the yellow line of Fig. 4 the initial drop of 10 ppmv for 1 ky and another 10 ppmv decrease for the subsequent 10 ky. The amplitude of this "rebound" also depends on how fast land carbon is released during deglaciation. Regrowth on land contributes a significant part of the subsequent decrease in CO_2 and temperature, but not the initial 10 ppmv drop as land is still releasing CO_2 at this time (Fig. 4).

The rapid CO_2 decrease levels off as both invasion/$CaCO_3$ "rebound" and boreal vegetation regrowth slow down after about 10 ky. Nonetheless, this is enough to produce a significant cooling and glaciation so that ice cover is at about 50% of its maximum extent, although the icesheets are only starting to grow in height, as indicated by ice volume (Fig. 3b), consistent with results from dynamic icesheet modeling (Marshall and Clark, 2002). As a result, despite the flatness in CO_2 over the next 15 ky, icesheet growth alone is able to drive further cooling. Interestingly, this continuing decrease in temperature at a time when CO_2 change slows down is also seen in the ice core data (Petit et al., 1999), and it is the period when CO_2 and temperature are least correlated both in the model and observations. However, such interpretation is cautioned because the detailed features may be sensitive to assumptions made in the model, and the observed features are also influenced by orbital forcing not considered here.

The last part of the glaciation again accelerates, although at a less rapid rate than glacial inception. During this period, Land carbon storage continues to increase but at slower and slower rate because boreal regrowth has stopped. This increase comes partly from continental shelf and partly from overall cooling-induced soil carbon storage (Fig. 3d). When icesheets grow to their maximum height, glacial burial carbon is ejected and start the deglacial positive feedbacks again, followed by another quasi-

CPD
2, 371–397, 2006

100 ky cycle.

It is worth emphasizing that oceanic CO_2 mechanisms, as represented by changes in SST in the model is always at work. Although the discussion above focuses on the major driving processes and key turning points in the model, the feedback between climate and carbon cycle on land and ocean, as well as the feedback between icesheets and climate all play important roles throughout a glacial-interglacial cycle.

5 Discussion

A key switch mechanism in the present theory from glacial to interglacial condition is the subglacial transport of glacial burial carbon. Besides large-scale ice flow, several mechanisms could act to flush out organic carbon buried under the icesheets at the height of glacial maximum. One such mechanism is through streams of meltwater at the base of an icesheet, as evidenced by eskers left behind by the great Northern Hemisphere icesheets, and more than half of the Laurentide and Fennoscandian periglacial sediment has been deposited by meltwater. Although it is probably difficult to distinguish in geological records meltwater events before and during deglaciation, it is possible that the basal melting at a glacial maximum before deglaciation also carried significant amount of organic carbon which may have left some evidence. Another mechanism involves fast flowing ice streams (MacAyeal, 1993) which could be very efficient at transporting and exposing large amount of carbon already near the edge of an icesheet. Some other processes such as iceshelf calving may also have played a role. However, these processes are poorly understood, and geological and modeling evidence show frozen bed under the ice domes and melting at outer areas at the last glacial maximum (LGM), followed by rapid inward melting during deglaciation (Kleman and Hattestrand, 1999; Marshall and Clark, 2002). In the absence of better understanding and availability of modeling tools, a rather simple treatment has been used here, with the caveat that it may not capture the details accurately of deglacial burial carbon release and the differences from termination to termination.

So far I have focused on the 100 ky cycle. The decay of icesheets over the 20 ky and 41 ky cycles may destroy some glacial burial carbon, but regrowth of the icesheets would bury them in a way similar to the major glacial inceptions on 100 ky timescale. Perhaps more importantly, such process is more likely to occur near the southern edge of the icesheets, thus impacting only a relatively small carbon pool. In contrast, basal transport is likely much more significant near glacial maximum than during the minor glacial periods because the slow growth in icesheet dynamics.

Interestingly, apart from the switch mechanisms at glacial maximum and interglacial discussed above, most of the major processes are the same during glaciation and deglaciation, such as CO_2-temperature and ice-albedo feedbacks, carbon storage/release on continental shelves, boreal carbon burial by ice and regrowth. A major difference is the different timescales as deglaciation lasts less than 10 ky while glaciation is an order of magnitude longer. This is mostly due to the asymmetry in icesheet melting and growth because melting is driven by radiative forcing while growth is limited by snow precipitation rate, and this fundamentally explains the "saw-tooth" structure of the observed 100 ky cycles. This icesheet growth/decay asymmetry has long been noted (Oerlemans, 1980), and the new insight here is its interaction with the carbon cycle.

Another noteworthy feature is the transient nature of interglacials. Vegetation regrowth, especially the "rebound" due to deep ocean invasion and carbonate compensation are on timescales from 1 ky to 10 ky, so interglacials are short, at least the part controlled by CO_2. In contrast, although there is no true equilibrium glacial maximum, the fact that icesheet growth is slow especially at large height when precipitation is minimum leads to significantly longer glacial maximum. The "rebound" and regrowth provide the switch from interglacial to glaciation. The relatively fast timescale of this switch is fundamental to the transient nature of CO_2 maximum, even if astronomical forcing happens to maintain high temperature.

6 Conclusions

Previous models that have been applied to long-term simulations tend to be simple, and it has been difficult to distinguish their relative merit (Roe and Allen, 1999). It is our hope that the mechanisms suggested here are sufficiently specific and the predictions are falsifiable. Marince C13 and carbonate data can provide major constraints on such model, but they need to be interpreted carefully together with other data such as ice core and terrestrial records in light of the transient nature of the phenomenon as well as new understanding of the glacial climate state. The modeling approach here is fairly comprehensive and represents a major effort in including relevant components with greater details.

The glacial-interglacial cycles simulated above are self-sustaining without external forcing. These quasi-100 ky cycles occur within certain plausible range of parameter values that need to be better identified perhaps in simpler models. Sensitivity experiments conducted so far indicate that they need relatively fast burial carbon release and carbon-climate feedback of sufficient strength. The key deglaciation switch due to glacial burial carbon ejection requires only basal flow to become substantial. This needs icesheets to grow large and long enough, without the requirement of increase in solar forcing, thus providing a potential explanation for the possible “causality problem”, i.e., observed deglaciation leads solar “forcing” (Winograd et al., 1992), as well as the “stage-11” problem (large deglaciation at a time of low solar variability). Orbital forcing is not included here so we can isolate a critical positive feedback process not considered before. Our findings do not exclude the role of Milankovitch orbital forcing, and most likely the carbon-climate-icesheet interaction and switch mechanisms identified here interact with orbital forcing to produce the complexity in the observed glacial-interglacial cycles.

Appendix A Model description

An Earth system model with balanced complexity in the components has been used to quantify the above theory. At present, it is not possible to run sophisticated GCMs continuously for such long-term integration. The physical climate components we use are "semi-empirical" by interpolating GCM-simulated climate time slices (Kutzbach et al., 1998) and reconstructed ices heet distributions for the last 21 ky (Peltier, 1994). The interpolation weighting factor is determined by time-dependent CO_2, ice cover and topography. The carbon cycle models for both land and ocean are mechanistic. A schematic diagram of the coupled model is shown in Fig. 5, and the details are given below.

A1 Atmosphere

The semi-empirical atmosphere model is interpolated between an interglacial maximum (Im) and a glacial maximum (Gm). Here the climate simulated by CCM1 (Kutzbach et al., 1998) for the Holocene (6 kBP) is used for Im while the LGM simulation is used for Gm. A single variable w is used to represent the climate state. For instance, temperature $T(x,t)$ can be computed as a linear interpolation between the two spatially varying extreme states $T_{Im}(x)$ and $T_{Gm}(x)$ simulated by CCM1 with w as the weighting factor:

$$T = wT_{Im} + (1-w)T_{Gm} \tag{A1}$$

where t is time and x represents the spatial dimensions, and w=$w(t)$ is a function of time only. Obviously, this approach does not represent spatial patterns that can not be expressed as linear combinations of the two extreme states. The related error would be larger near the icesheets than in other regions, but its overall effect should be of higher order for interaction with the carbon cycle.

The climate state variable w is determined by three independent factors as:

$$w = 0.5w_c + 0.3(1-w_i) + 0.2(1-w_h) \tag{A2}$$

where w_c is the contribution from the greenhouse effect of atmosphere CO_2, w_i is due to ice-albedo feedback of the icesheets, and w_h is related to atmospheric circulation changes caused by the topographical height of the icesheets. The CO_2 factor w_c is defined such that its value is larger (thus higher temperature) at higher CO_2, while w_i and w_h are defined such that their values are larger (lower temperature) at more ice cover and higher icesheets. The relative importance of these three factors are 50%, 30%, and 20%, based on various estimates of the relative roles of greenhouse gases and icesheets (Broccoli and Manabe, 1987; Lorius et al., 1990; Weaver et al., 1998). Other factors such as seaice, ocean circulation are fast changing and are treated as part of the physical atmosphere-ocean-land climate system which responds to greenhouse gas and icesheet forcing.

The contribution w_c is a function of instantaneous CO_2 interpolated between the model's interglacial equilibrium atmospheric CO_2 value CO_2^i of 272 ppmv and a glacial value CO_2^g of 190 ppmv:

$$w_c = \frac{CO_2 - {CO_2}^g}{{CO_2}^i - {CO_2}^g} \tag{A3}$$

A2 Dynamic vegetation and terrestrial carbon

The terrestrial carbon model Vegetation-Global-Atmosphere-Soil (VEGAS) simulates the dynamics of vegetation growth and competition among different plant functional types (PFTs). It includes 4 PFTs: broadleaf tree, needleleaf tree, cold grass, and warm grass. The different photosynthetic pathways are distinguished for C3 (the first three PFTs above) and C4 (warm grass) plants. Photosynthesis is a function of light, temperature, soil moisture and CO_2. Accompanying the vegetation dynamics is the full terrestrial carbon cycle starting from the allocation of the photosynthetic carbon into three vegetation carbon pools: leaf, root, and wood. After accounting for respiration, the biomass turnover from these three vegetation carbon pools cascades into a fast, an intermediate and finally a slow soil pool. Temperature and moisture dependent decomposition of these carbon pools returns carbon back into atmosphere, thus closes the terrestrial carbon cycle. A decreasing temperature dependence of respiration from fast to slow soil pools takes into account the effects of physical protection of organic carbon by soil particles below ground. The vegetation component is coupled to land and atmosphere through a soil moisture dependence of photosynthesis and evapotranspiration, as well as dependence on temperature, radiation, and atmospheric CO_2. The isotope carbon 13 is modeled by assuming a different carbon discrimination for C3 and C4 plants, thus providing a diagnostic quantity useful for distinguishing ocean and land sources and sinks of atmospheric CO_2. Competition between C3 and C4 grass is a function of temperature and CO_2 following Collatz et al. (1998)

The dynamic vegetation model is coupled to a physical land-surface model Simple-Land (SLand) (Zeng et al., 2000) which provides soil moisture and temperature, while evapotranspiration is coupled to the photosynthesis component of the vegetation model.

A3 Ocean

As noted above, factors such as seaice, ocean circulation are fast changing and are treated as part of the physical atmosphere-ocean-land climate system which responds to greenhouse gas and icesheet forcing, and they are therefore represented by the interpolation in the atmospheric model above. Since we are concerned about the interaction between carbon cycle and climate, we only need to represent the effects on carbon cycle of changes in the physical climate system.

A sea surface temperature anomaly T_o (relative to Im) is slaved to the atmosphere with a time delay of τ_o=100y:

$$\frac{dT_o}{dt} = \frac{(1-w)T_o^g - T_o}{\tau_o} \tag{A4}$$

where T_o^g=−6K is maximum glacial cooling. Zeng (2003) showed that a 4 K cooling in the ocean carbon model SUE leads to about 30 ppmv Im to Gm change, similar to a cooler-than-CLIMAP scenario supported by recent studies (Ridgwell, 2001). Since it is beyond the scope here to include all the ocean mechanisms, a change of ocean temperature by 6 K was chosen to obtain a total ocean-driven change of about 55 ppmv, a value on the low side of which the major oceanic mechanisms can explain.

The ocean carbon cycle model SUE (Ridgwell, 2001) simulates both the ocean CO_2 mixing and $CaCO_3$ sediment dissolution processes, as well as carbon 13. The version used here consists of 16 horizontal regions covering the major oceanic sub-basins and 8 layers in the vertical, forced by the fields of modern circulation, salinity, etc. All the active changes on glacial-interglacial cycles are represented by changes in sea surface temperature as discussed above.

A major caveat is that this approach will not resolve significant timing differences of different ocean CO_2 mechanisms. For instance, the earlier CO_2 release may be caused by glacial dust fertilization while the sea-level related changes such as coral reef hypothesis would occur several thousand years later. Ocean surface temperature changes took place throughout deglaciation, thus piggybacking the other active ocean changes on it should capture the overall effects. Future research will include other active ocean mechanisms in a more realistic way. It is worth noting that, the passive oceanic buffering effects in response to terrestrial changes are always considered, including the multiple time scales associated with deep ocean circulation and sediment carbonate compensation.

A4 Icesheet dynamics

This semi-empirical model is not mechanistic, but nonetheless represents several major icesheet processes such as the asymmetry in time scale during decay and growth, and is constrained by the observed changes over the last 21 ky.

Ice cover change is assumed to follow temperature change with a delay of τ_i=100y:

$$\frac{dw_i}{dt} = \frac{1 - w - w_i}{\tau_i} \tag{A5}$$

CPD

2, 371–397, 2006

Glacial cycles triggered by burial carbon release

N. Zeng

EGU

The weighting factor w_i could then be used to interpolate the ice cover. However, unlike the straightforward interpolation for temperature and precipitation (which can also be extrapolated), ice cover is either 0 or 1. Ice cover "interpolation" is therefore done by spreading (glaciation) or shrinking (deglaciation) the ice cover data (Peltier, 1994) at 1 ky time resolution based on the information of w_i. Thus the Laurentide icesheet can not spread further south than at LGM even if the climate gets cooler. Another consequence of these lower and upper limits on icesheet is that when climate is outside the LGM and Holocene bound (w less than 0 or great than 1), further climate change will come only from CO_2 greenhouse effect. This is a limitation of the semi-empirical model but not a major drawback as the model will be applied only to the Pleistocene when LGM was the coldest period. On the warmer side, since Antarctica and Greenland had no major change in ice-covered area during Pleistocene, only regions such as the high arctic Canadian islands may have changed significantly but their small area should not have a major impact on our results. In addition, as a posteriori justification, the model simulated a CO_2 range of 190–280 ppmv, so that the interpolation is only slightly out of range on the warm side because w_c is interpolated using CO_2 range of 190–272 ppmv (Eq. A3).

Once a place is ice covered, ice thickness $h(x)$ grows linearly towards a potential value $w_i h_{\max}$ at a time scale τ_h:

$$\frac{dh}{dt} = \frac{w_i h_{\max}}{\tau_h} \tag{A6}$$

where $h_{\max}(x)$ is the ice thickness of the difference of the observed LGM and Holocene values (Peltier, 1994), and τ_h (in ky) is:

$$\tau_h = \begin{cases} 4, & \text{ice decay} \\ 15(1-w_h) + 40w_h, & \text{ice growth} \end{cases} \tag{A7}$$

Whether the icesheets are in a decay or growth phase depends on whether global ice volume is decreasing or increasing (below). Furthermore, if ice cover becomes zero at any specific place, ice thickness is immediately set to zero. Icesheet melting is fast

CPD
2, 371–397, 2006

during decay, thus the 4 ky time scale. The icesheet growth is set between 15 ky and 40 ky with slower rate at higher icesheet to account for the fact that snowfall decreases at higher altitude. The timescales, both at growth and decay, represents the rates at maximum climate forcing so that the actual glaciation and deglaciation would take longer. And not surprisingly, the duration of the simulated glacial-interglacial cycles are sensitive to especially the growth time scales.

The ice topography factor w_h is defined as relative ice volume.

$$w_h = V_i / V_{i\,\max} \tag{A8}$$

where V_i is the ice volume of the changing icesheets, i.e., a spatial integral of ice thickness h, while $V_{i\,\max}$ is its maximum value. Note that these are all changes relative to an interglacial value so that w_h goes from 0 to 1 when ice grows from Holocene maximum to LGM. And sea level change is also proportional to w_h. Then icesheet topography (altitude at the surface of the icesheet) relative to sea level $h_s(x)$ is computed as:

$$h_s = h_{s\,\min} + (h_{s\,\max} - h_{s\,\min}) w_h \tag{A9}$$

where $h_{s\,\max}(x)$ and $h_{s\,\min}(x)$ are the observed height at LGM and Holocene (Peltier, 1994), respectively.

A5 Subglacial transport of organic carbon

When icesheet grows to substantial height, subglacial basal flow becomes significant, especially when melting occurs at the base. The transport of glacial burial carbon by basal flow is at the center of the current theory. However, the processes of subglacial transport of sediment are poorly understood, and process-based modeling is being attempted only very recently (Hildes et al., 2004).

Besides large-scale ice flow, several mechanisms could act to flush out organic carbon buried under the icesheets at the height of glacial maximum. One such mechanism is through streams of meltwater at the base of an icesheet, as evidenced by eskers left behind by the great Northern Hemisphere icesheets. More than half of the sediment deposited by Laurentide icesheet may have been carried by these subglacial rivers. It is well known that meltwater from the Laurentide icesheet flew into the Gulf of Mexico through the Mississippi river basin during deglaciation. And it is likely that the basal melting at a glacial maximum before deglaciation also carried significant amount of organic carbon which may have left some evidence. Another mechanism involves the fast moving ice streams (MacAyeal, 1993) which could be very efficient at transporting and exposing large amount of carbon already near the edge of an icesheet. Many other icesheet instability mechanisms may also play a role. Geological and icesheet modeling evidence show frozen bed under the ice domes and melting at outer areas at LGM, followed by rapid melting during deglaciation (Kleman et al., 1999; Marshall and Clark, 2002). In the absence of better understanding and availability of modeling tool, a rather simple treatment is used here, with the caveat that it may not capture the details accurately of deglacial burial carbon release and the differences from termination to termination.

Transport of glacial sediment including burial carbon is modeled as:

$$v = -C_{sl} h |\nabla h_s|^2 \nabla h_s + v_0 \tag{A10}$$

where v is the velocity at the ice-sediment boundary, and the full vertical profile is assumed quadratic with v as the top boundary condition and zero as the lower sediment-bedrock boundary condition. The first term on the rhs is a large-scale flow (Greve, 1997), and the second term v_0 represents additional transport at deglaciation of the burial organic carbon towards the edge of the icesheets at a speed increasing from zero to 8×10^{-6} m s^{-1} (250 m y^{-1}) within 3000 years. v_0 is nonetheless very important for our model behavior, as the speed at which the glacial burial carbon is transported out of the icesheet (therefore how fast it is released back into the atmosphere) is critical for initiating the positive feedbacks at deglaciation. The transport starts when ice volume grows to the maximum value (w_h=1). This also signals the beginning of deglaciation. The treatment here can thus only be considered an assumption, or at most a highly simplified representation rather than detailed mechanistic prediction.

After the burial carbon being re-exposed to the atmosphere, it is decomposed at a time scale of 100 year at 25°C and slower at lower temperature.

A6 Treatment of carbon on continental shelves

During the glacial-interglacial cycles, sea level rises and falls as water is drawn to form ice on land and vise versa. Sea level is predicted using the ice volume factor w_h, and a land-sea mask is determined at each time step according to the topographical information h_s above. The continental shelf area exposed at lower sea level grows vegetation and accumulates carbon, modeled dynamically as climate changes. The shelf carbon was subsequently submerged and released back into the atmosphere at deglaciation. The time scale for the decomposition of the submerged carbon was set at 300 y at 25°C.

Acknowledgements. I am grateful to W. Ruddiman for insightful comments. The ocean carbon model was kindly provided by A. Ridgwell. The project was in part supported by NSF grant ATM-0328286, NOAA grants NA04OAR4310091 and NA04OAR4310114.

References

Archer, D., Kheshgi, H., and Maier-Reimer, E.: Multiple timescales for neutralization of fossil fuel CO2, Geophys. Res. Lett., 24(4), 405–408, 1997.

Archer, D., Winguth, A., Lea, D., and Mahowald, N.: What caused the glacial/interglacial atmospheric pCO(2) cycles?, Rev. Geophys., 38, 159–189, 2000:

Broccoli, A. J. and Manabe, S.: The influence of continental ice, atmospheric CO2, and land albedo on the climate of the last glacial maximum, Clim. Dyn., 1, 87–99, 1987.

Broecker, W. S. and Henderson, G. M.: The sequence of events surrounding Termination II and their implications for the cause of glacial-interglacial CO2 changes, Paleoceanography, 13, 352–364, 1998.

Collatz, G. J., Berry, J. A., and Clark, J. S.: Effects of climate and atmospheric CO2 partial pressure on the global distribution of C-4 grasses: present, past, and future, Oecologia, 114, 441–454, 1998.

Curry, W. B., Duplessy, J.-C., Labeyrie, L. D., and Shackleton, N. J.: Changes in the distribution of $delta^{13}$C of deep water CO2 between the last glacial and the Holocene, Paleoceanography, 3, 317–341, 1988.

EPICA community members: Eight glacial cycles from an Antarctic ice core, Nature, 429, 623–628, 2004.

Gildor, H. and Tziperman, E.: Physical mechanisms behind biogeochemical glacial-interglacial CO2 variations, Geophys. Res. Lett., 28(12), 2421–2424, 2001.

Greve, R.: A continuum-mechanical formulation for shallow polythermal icesheets, Phil. Trans. R. Soc. Lond., A, 355, 921–974, 1997.

Hays, J. D., Imbrie, J., and Shackleton, N. J.: Variations in the Earth's orbit: Pacemakers of the ice ages, Science, 194, 1121–1132, 1976.

Hildes, D. H. D., Clarke, G. K. C., Flowers, G. E., and Marshall, S. J.: Subglacial erosion and englacial sediment transport modelled for North American ice sheets, Quaternary Sci. Rev., 23(3), 409–430, 2004.

Imbrie, J., Berger, A., Boyle, E. A., et al.: On the Structure and origin of major glaciation cycles. 2. The 100,000-year cycle, Paleoceanography, 8(6), 699–735, 1993.

Kleman, J. and Hattestrand, C.: Frozen-bed Fennoscandian and Laurentide ice sheets during the Last Glacial Maximum, Nature, 402(6757), 63–66, 1999.

Kutzbach, J., Gallimore, R., Harrison, S., Behling, P., et al.: Climate and biome simulations for the past 21,000 years, Quaternary Sci. Rev., 17, 473–506, 1998.

Lorius, C., Jouzel, J., Raynaud, D., et al.: The ice-core record – climate sensitivity and future greenhouse warming, Nature, 347(6289), 139–145, 1990.

MacAyeal, D. R.: Binge/purge oscillations of the Laurentide Ice Sheet as a cause of the North Atlantic Heinrich events, Paleoceanography, 8, 775–784, 1993.

Marshall, S. and Clark, P.: Basal temperature evolution of North American ice sheets and implications for the 100-kyr cycle, Geophys. Res. Lett., 29, doi:10.1029/2002GL015192, 2002.

Oerlemans, J.: Model experiments on the 100,000-yr glacial cycle, Nature, 287, 430–432, 1980.

Paillard, D. and Parrenin, F.: The Antarctic ice sheet and the triggering of deglaciations, Earth Planet. Sci. Lett., 227 (3–4), 263–271, 2004.

Peltier, W. R.: Ice age paleotopography, Science, 265, 195–201, 1994.

Petit, J. R., Jouzel, J., Raynaud, D., et al.: Climate and atmospheric history of the past 420,000 years from the Vostok ice core, Antarctica, Nature, 399, 429–436, 1999.

Ridgwell, A. J.: Glacial-interglacial perturbations in the global carbon cycle, PhD thesis, Univ. of East Anglia at Norwich, UK, available at: http://tracer.env.uea.ac.uk/e114/ridgwell_2001.pdf, 2001.
Roe, G. H. and Allen, M. R.: A comparison of competing explanations for the 100,000-year ice age cycle, Geophys. Res. Lett., 26(15), 2259–2262, doi:10.1029/1999GL900509, 1999.
Ruddiman, W. F.: Orbital insolation, ice volume, and greenhouse gases, Quat. Sci. Rev., 22(15–17), 1597–1629, 2003.
Saltzman, B. and Maasch, K. A.: Carbon cycle instability as a cause of the late Pleistocene ice age oscillations: Modeling the asymmetric response, Global Biogeochem. Cycles, 2(2), 177–185, 1988.
Sigman, D. M. and Boyle, E. A.: Glacial/interglacial variations in atmospheric carbon dioxide, Nature, 407, 859–869, 2000.
Smith, H. J., Fischer, H., Wahlen, M., et al.: Dual modes of the carbon cycle since the Last Glacial Maximum, Nature, 400, 248–250, 1999.
Spero, H. J., Bijma, J., Lea, D. W., and Bemis, B. E.: Effect of seawater carbonate concentration on foraminiferal carbon and oxygen isotopes, Nature, 390(6659), 497–500, 1997.
Spero, H. J. and Lea, D. W.: The cause of carbon isotope minimum events on glacial terminations, Science, 296, 522–525, 2002.
Weaver, A. J., Eby, M., Augustus, F. F., et al.: Simulated influence of carbon dioxide, orbital forcing and ice sheets on the climate of the Last Glacial Maximum, Nature, 394(6696), 847–853, 1998.
Winograd, I. J., Coplen, T. B., Landwehr, J. M., et al.: Continuous 500,000-year climate record from vein calcite in Devils-Hole, Nevada, Science, 258(5080), 255–260, 1992.
Wunsch, C.: Quantitative estimate of the Milankovitch-forced contribution to observed Quaternary climate change, Quat. Sci. Rev., 23(9–10), 1001–1012, 2004.
Zeng, N., Neelin, J. D., and Chou, C.: A quasi-equilibrium tropical circulation model–implementation and simulation, J. Atmos. Sci., 57, 1767–1796, 2000.
Zeng, N.: Glacial-Interglacial Atmospheric CO2 Changes – The Glacial Burial Hypothesis, Adv. Atmos. Sci., 20, 677–693, 2003.

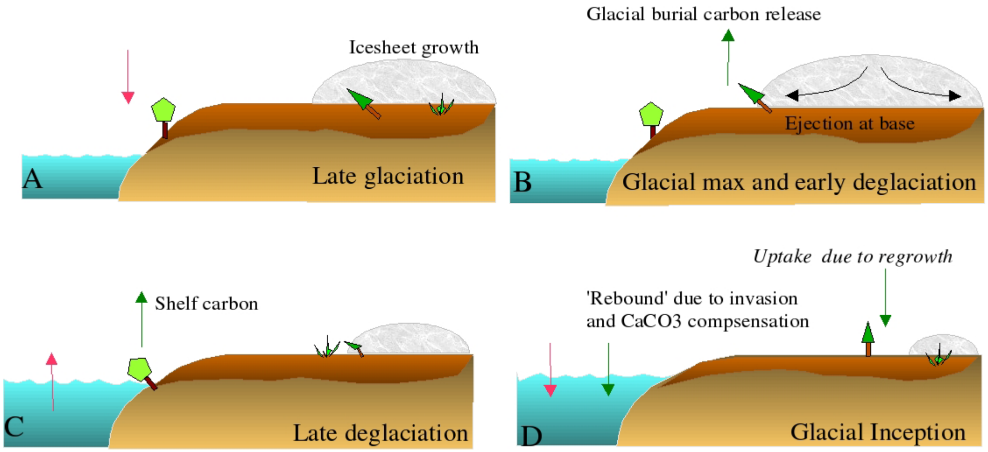

Fig. 1. Conceptual diagram of proposed carbon-climate-icesheet feedback mechanism during some major stages of the 100 ky cycle: **(a)** late glaciation, cold climate enhanced by feedbacks such as CO_2-temperature and ice-albedo-topography, with about 500 Gt carbon accumulated under the icesheets; **(b)** glacial maximum and early deglaciation with basal ejection of glacial burial carbon and subsequent CO_2 release as the trigger; **(c)** late deglaciation with also continental shelf carbon and oceanic CO_2 release; **(d)** glacial inception, initiated by "rebound" from rapid deglacial land CO_2 release due to deep ocean invasion and $CaCO_3$ compensation, and vegetation regrowth. Red arrows indicate fluxes due to other oceanic mechanisms such as SST change.

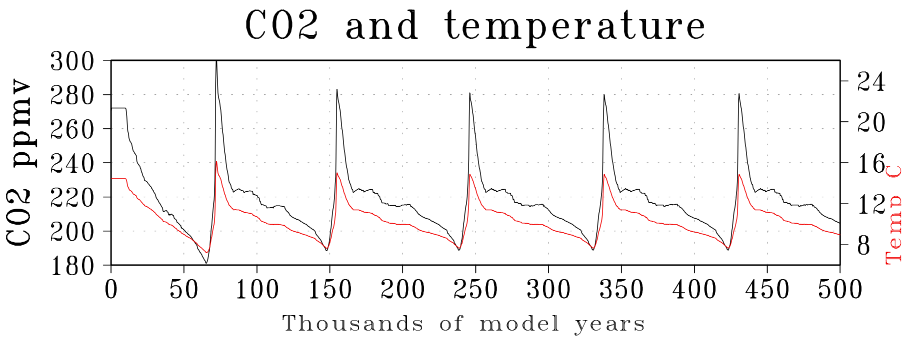

Fig. 2. Quasi-100 ky cycles simulated by the coupled model. The first two cycles are in adjustment with the model spinup and an artificial CO_2 sink, followed by quasi-steady cycles with a period of 93 ky. The glacial to interglacial amplitudes are 90 ppmv in CO_2, and 6°C in temperature.

CPD

2, 371–397, 2006

Glacial cycles triggered by burial carbon release

N. Zeng

EGU

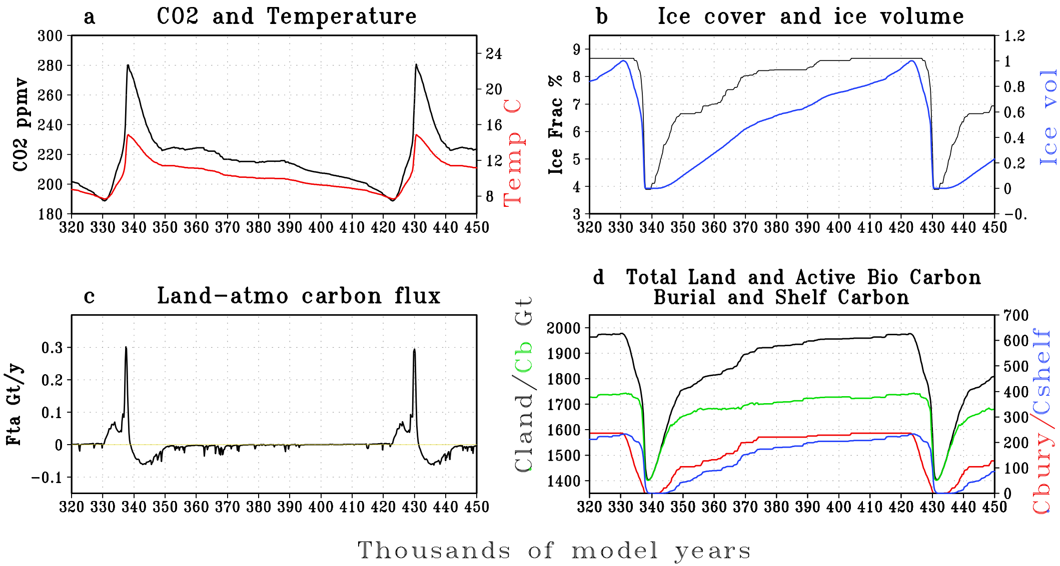

Fig. 3. Various model simulated global total or average quantities: **(a)** Atmospheric CO_2 (black) and temperature (red); **(b)** Ice covered area as percentage of world total (black), and ice volume (blue) normalized between 0 (Holocene) and 1 (LGM); **(c)** Land-atmospheric carbon flux (F_{ta}); note the double peaks at deglaciation due to glacial burial carbon and continental shelf carbon release; **(d)** Carbon pools for total land (C_{land}, black), active biosphere (C_b, green), glacial burial (C_{bury}, red) and continental shelves (C_{shelf}, blue).

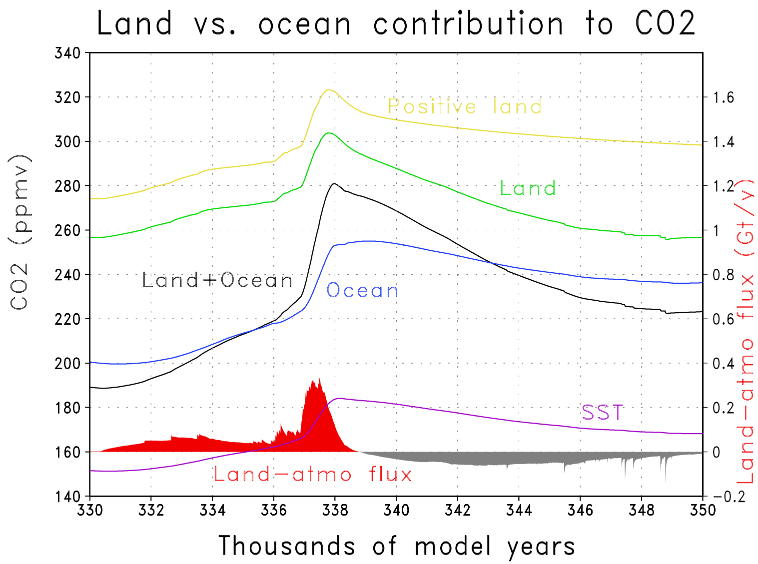

Fig. 4. CO_2 change during deglaciation and glacial inception from 3 sensitivity experiments in which the atmosphere-ocean carbon model was forced by: 1. ocean changes only (blue line; using SST cooling of 6°C at glacial max as a surrogate of all active ocean mechanisms, with SST in purple; this SST "piggybacking" may not resolve the timing differences in different ocean mechanisms); 2. land flux forcing only (green, with land-atmo carbon flux shown as red-gray shaded curve; note the double peaks at deglaciation due to the earlier glacial burial carbon and later continental shelf carbon release); 3. the positive part of land flux forcing only (yellow), i.e., the negative flux (shaded in gray) was set to zero. The forcing SST and land flux are from the fully coupled run whose CO_2 change is shown in black. The "land" only curve is shifted upward because of the lack of oceanic forcing, and the "positive land" curve is further shifted because there is no negative flux to balance the input to the atmosphere-ocean system. Note the CO_2 drawdown of about 10 ppmv at early glacial inception even in the "positive land" flux only case, despite the lack of any CO_2 uptake by land. This is caused by a "rebound" from the high interglacial CO_2 as land-originated carbon is absorbed into deep ocean by thermohaline circulation and $CaCO_3$ compensation.

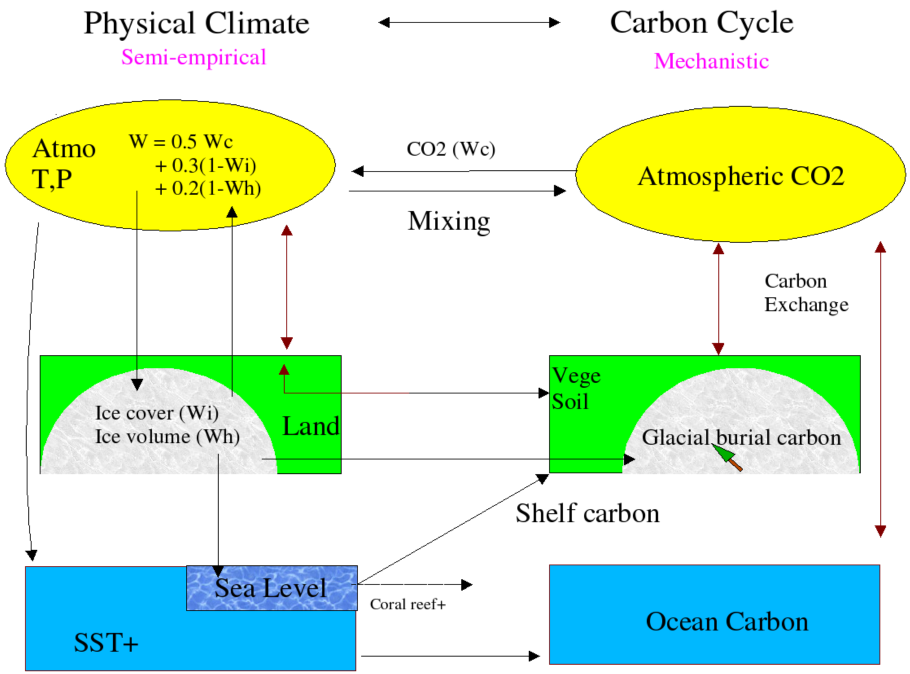

Fig. 5. Schematic diagram of the modeling approach. Note the full interactiveness (prognostic) of physical climate including icesheet and carbon cycle. While the carbon cycle components are process based, the physical climate components are semi-empirical based on GCM timeslice simulations and icesheet reconstruction. A strong SST change is used as a surrogate for all the other active oceanic mechanisms.